A Quantitative Comparative Study of Efficiency for Battery-Ultracapacitor Hybrid Systems

Chen Zhao, He Yin
Univ. of Michigan-Shanghai Jiao Tong Univ. Joint Institute,
Shanghai Jiao Tong University,
Shanghai, P. R. China
Email: chenzhaosjtu@gmail.com
yyy@sjtu.edu.cn

Zhongping Yang
School of Electrical Engineering
Beijing Jiao Tong University,
Beijing, P. R. China
Email: zhpyang@bjtu.edu.cn

Chengbin Ma*[1,2]
1. Univ. of Michigan-Shanghai Jiao Tong Univ. Joint Institute,
2. School of Mechanical Engineering,
Shanghai Jiao Tong University,
Shanghai, P. R. China
Email: chbma@sjtu.edu.cn

***Abstract*—This paper provides a quantitative and comparative study on efficiencies of a battery semi-active hybrid energy storage system (HESS) and a battery-only system. The discussion is based on the equivalent series resistance (ESR) circuit models and a pulsed current load. It is theoretically proved that the efficiency difference between the two systems depends on the variance of the load current, the average load current, and the internal resistance of the battery pack. A threshold variance is then accurately derived, above which the battery semi-active HESS becomes more energy efficient. This threshold decreases with an increasing internal resistance of the battery pack and/or a decreasing average load current. Therefore, the best usage of ultracapacitors is to combine with batteries designed for low cost (i.e. a large internal resistance), and supply the dynamic part of a current load with a high peak-to-average ratio. Finally, JC08 driving cycle-based simulation validates the theoretical analysis.**

***Index Terms*—Battery, Ultracapacitor, Hybrid energy storage system, Efficiency, Equivalent series resistance circuit**

I. Introduction

Portable electronic devices, telecommunication systems, and electric vehicles share a common dynamic power requirement. For the widely used battery-based energy storage systems, the dynamic load current with high peak-to-average ratio shortens the battery service time due to the rate capacity effect in batteries [1]. It is well-known now that by combining with ultracapacitors, the peak current of batteries can be reduced, and the power capability of the overall energy storage system can also be improved. This is because that ultracapacitors have a much higher power density and a better reliability compared to batteries [2].

In general, battery-ultracapacitor hybrid energy storage systems (HESSs) can be classified into three types: passive, semi-active, and fully active hybrids [3]. In the passive HESS, batteries and ultracapacitors are directly connected in parallel. The benefit of a passive HESS over a battery-only system was shown in the case that the load pulse duty is small, and the load pulse rate is higher than the system eigen-frequency [4], [5]. The Ragone plots based studies show that the deliverable energy of the passive HESS is increased when both the discharged energy and duty cycle of the pulse load are small [6], [7]. For active HESSs, DC-DC converters are used to regulate the energy flow among batteries, ultracapacitors, and the load. It was shown that the power capability of an active HESS was higher than that of both passive HESS and battery-only system, but might lead to more energy loss [8]. Many energy management strategies have been proposed in order to maximize the efficiency of the battery-ultracapacitor HESSs. An optimal-control approach was discussed and implemented using Neural Networks to achieve a higher efficiency than the battery-only system [9], [10]. The rule-based approaches were shown to be suitable for the control of the HESSs [11]–[13]. Model predictive control and Markov process were applied in order to handle various constraints and predict future load demands [13], [14]. The trade-off between battery protection and the minimization of energy loss has been addressed by using a multi-objective optimization approach [15], [16]. Meanwhile, it is ideal to let batteries satisfy the average load demand (ALD) (i.e., a constant current), and thus ultracapacitors provide all the dynamic load current [8], [17], [18]. Without considering physical limitations, the ALD-based control is the best for the battery-ultracapacitor HESSs.

As to the knowledge of the authors, there is still a lack of a quantitative comparison between a battery-ultracapacitor HESS and a battery-only system. This comparative study is important to determine the best usage of the HESS. Therefore, this paper aims to provide a detailed quantitative and comparative study on the efficiencies of a battery-ultracapacitor HESS and a battery-only system. The battery semi-active topology is chosen here because this topology enables batteries to work at the point close to the average power/current [3]. The efficiency analysis of the two systems is based on their equivalent series resistance (ESR) circuit models and a pulsed current load. In the battery semi-active HESS, the average load current is supplied by the battery pack through the DC-DC converter. The efficiencies of the two systems are then accurately calculated and compared with varied average load currents, internal resistances of the battery pack, and the variances of the load demand. Both the theoretical analysis and simulation result justify that the battery-ultracapacitor HESS works best with low-cost batteries (i.e. a large internal resistance) and a load demand with a high peak-to-average

978-1-4799-4033-2/14/$31.00 ©2014 IEEE

ratio.

II. ESR-based Efficiency Analysis

A. Pulsed Current Load

For a theoretical discussion, the pulsed current load is used to represent a dynamic power requirement [3]. Fig. 1 shows that the pulsed current load can be decomposed into two components, constant average current $I_{l,a}$ and dynamic current $i_{l,d}$. The average load current $I_{l,a}$ and the variance of the load current $\mathrm{Var}(i_l)$ are defined in (1) and (2):

$$\begin{aligned} I_{l,a} &= DI_{l,max} + (1-D)I_{l,min}, && (1) \\ \mathrm{Var}(i_l) &= (I_{l,max} - I_{l,a})(I_{l,a} - I_{l,min}), \\ &= I_{l,dp}I_{l,dn}, && (2) \end{aligned}$$

where $I_{l,max}$ and $I_{l,min}$ are the maximum and minimum load currents, respectively. D is the duty cycle of the pulsed load. $I_{l,dp}$ and $I_{l,dn}$ are the dynamic part of the load current during DT and $(1-D)T$, respectively.

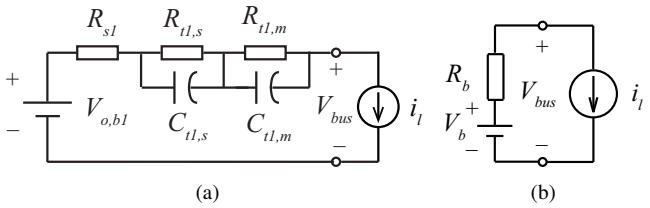

Fig. 2. Model of battery-only system and its ESR circuit. (a) Model of the battery-only system. (b) ESR circuit for the battery-only system.

B. Efficiency Analysis and Comparison

For a comparison purpose, in the following subsections, the efficiencies of the battery semi-active HESS and the battery-only system are accurately derived under a same pulsed current load.

1) Battery-only System: In the battery-only system, the battery pack (4S2P) are directly connected to the load, as shown in Fig. 2(a). Because the electrochemical battery model is mainly used for battery design, it is too complicated to be used in system level analysis. The equivalent circuit model for the NiMH and lithium ion batteries is used to analyze the efficiency of the lithium ion battery pack here [19]. The 4S2P here means that four cells are in series and two strings of these four cells are in parallel. The resistor R_{s1} and open circuit voltage (OCV) $V_{o,b1}$ of the battery pack are represented by six-order polynomials:

$$\begin{aligned} V_{o,b1} &= a_0 + a_1x + a_2x^2 + ... + a_6x^6, && (3) \\ R_{s1} &= b_0 + b_1x + b_2x^2 + ... + b_6x^6, && (4) \end{aligned}$$

where x is a specific state of charge (SOC) [20]. The two RC networks with different time constants, $\tau_s = R_{t1,s}C_{t1,s}$, $\tau_m = R_{t1,m}C_{t1,m}$ model the battery transient voltage responses in seconds and minutes ranges, respectively [20]. The parameters of the battery pack are determined experimentally by using the fast averaging method [21] and listed in Table I. Fig. 2(b) shows the ESR circuit of the battery-only system [refer to AppendixA]. Then the efficiency of the battery-only system under the pulsed current load can be calculated as

$$\eta_{bo} = 1 - \frac{I_{l,a}^2 R_b + I_{l,dp}I_{l,dn}R_b}{V_{o,b1}I_{l,a}}. \quad (5)$$

2) Battery Semi-active HESS: As shown in Fig. 3(a), the ultracapacitor pack is directly connected to the load and a DC-DC converter is placed between the battery pack and the load. For comparison purpose, the voltage of the ultracapacitor pack is set to be equal to that of the battery pack (4S2P) in the battery-only system. The advantage of the battery semi-active HESS is that the voltage of the battery pack does not have to match the DC bus voltage. In the proposed experimental setup, the battery pack (2S4P) is chosen so that a current-mode controlled boost converter is employed in the battery semi-active HESS. Similarly, the equivalent circuit model is used to represent the dynamics of the battery pack (2S4P). Eight cells are connected in series in the ultracapacitor pack. For the purpose of the system level analysis, the first-order electrical model is used to represent the dynamics of the ultracapacitor pack [22]. The capacitance of the ultracapacitor pack C_u depends on the OCV of the ultracapacitor pack, $V_{o,u}$. Resistor R_{sc} corresponds to the internal resistance of the ultracapacitor pack, and resistor R_{pc} models the leak current [22]. The parameters of the ultracapacitor pack are determined experimentally by using the pulsed current test [23]. The parameter values of the HESS in Fig. 3(a) are also listed in Table I.

Fig. 3(b) shows the ESR circuit of the battery semi-active HESS, where "*" denotes the ESR for each component in terms of energy loss. The calculation of parameters in Fig. 3(b) is explained in the Appendix A. In this paper, the average load demand (ALD) control is applied in the battery semi-active HESS. In the control, the output current of the DC-DC converter i_d is equal to the average current of the load $I_{l,a}$. The ultracapacitor pack supplies the entire dynamic part of the load current $i_{l,d}$. The ALD-based control is considered to be optimal for the HESS assuming that there is no physical limitations [18]. Similarly, the efficiency of the battery semi-active HESS can be written as

$$\eta_{bs} = 1 - \frac{I_{l,a}^2 (R_b^* + R_d^*) + I_{l,dp}I_{l,dn}R_u^*}{V_{o,u}I_{l,a} + I_{l,a}^2 (R_b^* + R_d^*)}. \quad (6)$$

III. Quantitative Comparison

For a comparable performance, the OCV of the battery pack in the battery-only system $V_{o,b1}$ is equal to that of the ultracapacitor pack $V_{o,u}$ in the HESS. By combining (2)(5)(6), the difference between the efficiency of the battery semi-active HESS and that of battery-only system, $\Delta\eta$, can be derived as

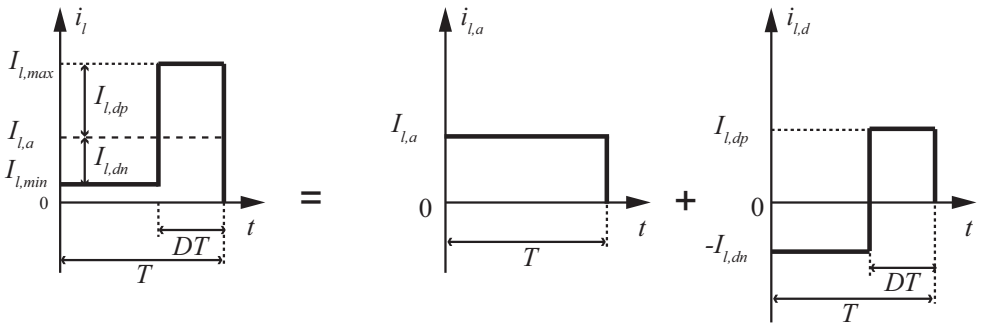

Fig. 1. Decomposition of the pulsed current load during a single period T.

TABLE I
PARAMETERS FOR THE BATTERY PACK, THE DC-DC CONVERTER, AND THE ULTRACAPACITOR PACK

Battery Pack (4S2P)							
a_0	12.38	a_1	29.02	a_2	-129.51	a_3	299.09
a_4	-366.81	a_5	231.77	a_6	-59.23	b_0	0.49
b_1	-4.72	b_2	28.51	b_3	-83.27	b_4	125.62
b_5	-94.10	b_6	27.67	$R_{t1,s}$	29 mΩ	$C_{t1,s}$	5300 F
$R_{t1,m}$	8 mΩ	$C_{t1,m}$	3000 F				
Battery Pack (2S4P)							
a_0	6.38	a_1	11.99	a_2	-51.75	a_3	116.28
a_4	-138.41	a_5	85.11	a_6	-21.23	b_0	0.13
b_1	-1.29	b_2	7.77	b_3	-22.50	b_4	33.64
b_5	-25.02	b_6	7.32	$R_{t2,s}$	15mΩ	$C_{t2,s}$	10000 F
$R_{t2,m}$	10 mΩ	$C_{t2,m}$	2500 F				
Ultracapacitor Pack (8S1P)							
C_u	(2.17$v_{o,u}$+188.6) F			R_{sc}	10 mΩ	R_{pc}	3 kΩ
DC-DC Converter							
R_{MOS}	5 mΩ	L	200 μH	R_L	100 mΩ	C_{out}	2000 μF

follows:

$$\begin{aligned}\Delta\eta &= \eta_{bs} - \eta_{bo} \\ &= \frac{I_{l,a}\left[R_b - (R_b^* + R_d^*)\left(1 - \frac{R_b I_{l,a}}{V_{o,u}}\right)\right]}{V_{o,u} + I_{l,a}\,(R_b^* + R_d^*)} \\ &\quad + \frac{\mathrm{Var}(i_l)\left[R_b + (R_b^* + R_d^*)\,\frac{R_b I_{l,a}}{V_{o,u}} - R_u^*\right]}{I_{l,a}\left[V_{o,u} + I_{l,a}\,(R_b^* + R_d^*)\right]}. \quad (7)\end{aligned}$$

From (7), in order to have a positive $\Delta\eta$, the variance of the pulsed current load $\mathrm{Var}(i_l)$ should satisfy

$$\mathrm{Var}(i_l) > \mathrm{Var}(i_l)_{th}, \quad (8)$$

where the threshold, $\mathrm{Var}(i_l)_{th}$, is

$$\mathrm{Var}(i_l)_{th} = \frac{I_{l,a}^2\left[(R_b^* + R_d^*)\left(1 - \frac{R_b I_{l,a}}{V_{o,u}}\right) - R_b\right]}{R_b + (R_b^* + R_d^*)\,\frac{R_b I_{l,a}}{V_{o,u}} - R_u^*}. \quad (9)$$

It shows that if the variance of the pulsed current load, $\mathrm{Var}(i_l)$, is larger than $\mathrm{Var}(i_l)_{th}$, the efficiency of the battery semi-active HESS is higher than that of the battery-only system.

Fig. 4 shows the efficiencies of the battery-only system and battery semi-active HESS when the $I_{l,a}$ and the SOCs of the battery packs in two systems are set to be 2 A and 50%, respectively. Because the maximum charging and discharging currents of the battery pack in battery-only system are 5 A and 10 A, the current ranges of the $I_{l,max}$ and $I_{l,min}$ are set to 2–10 A and -5–0 A, where the negative current corresponds to the charging and vice versa. Fig. 4(a) shows that the efficiencies of two systems both decrease when $I_{l,max}$ or $I_{l,min}$ increases. The efficiency curves of the two systems are replotted in Fig. 4(b) with respect to the variance of the pulsed current load $\mathrm{Var}(i_l)$ [refer to (2)]. It shows that η_{bs} is higher than η_{bo} when $\mathrm{Var}(i_l)$ is larger than 10.7. It is consistent with the condition in (8) because $\mathrm{Var}(i_l)_{th}$ is 10.7. The efficiency drop caused by the increasing $\mathrm{Var}(i_l)$ in the battery semi-active HESS is less than that of the battery-only system. It is because that the dynamic part of the load current is entirely supplied by the high-efficiency ultracapacitors in the HESS.

Equation (9) shows that $\mathrm{Var}(i_l)_{th}$ relates to various parameters of the two systems. Fig. 5 shows the tornado diagram representing the impact of various parameters on $\mathrm{Var}(i_l)_{th}$. It can be seen that $I_{l,a}$ and R_b are the top two sensitive factors. In the sensitivity analysis, the same type of batteries are used in the two systems. The resistance of the battery pack (2S4P)

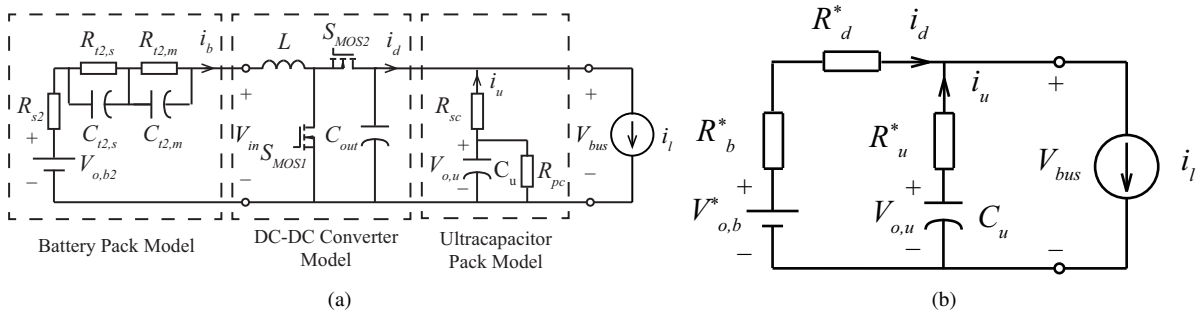

Fig. 3. Model of battery semi-active HESS and its ESR circuit. (a) Models of battery pack, DC-DC converter, and ultracapacitor pack in HESS. (b) ESR circuit for the battery semi-active HESS.

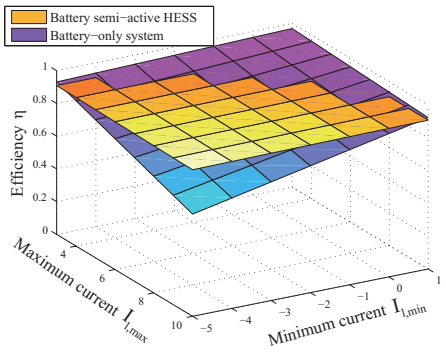

Fig. 4. Efficiency maps of the battery semi-active HESS and the battery-only system when $I_{l,a}$ =2 A and the SOCs for the battery packs are both 50%.(a) Efficiency as a function of $I_{l,max}$ and $I_{l,min}$. (b) Efficiency as a function of Var(i_l).

R_{s2} in the battery semi-active HESS is assumed to be $1/4$ of that of the battery pack (4S2P), R_{s1}, in the battery-only system. From Appendix A, R_{s1} is equal to R_b in (9). The ranges of the parameters in the systems are shown in Table II. The range of $I_{l,a}$ is determined based on the power rating of the DC-DC converter. The range of $V_{o,b1}$ is the voltage range of the battery pack (4S2P) in the battery-only system. The ranges of R_b and R_u^* are determined based on their thermal dependence. The influences of the $I_{l,a}$ and R_b are analyzed as follows.

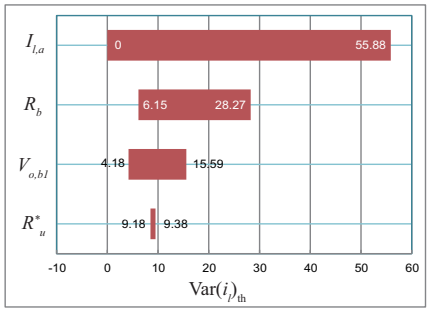

Fig. 5. Tornado diagram for the sensitivity analysis on Var$(i_l)_{th}$.

TABLE II
RANGES OF THE PARAMETERS

Parameter	$I_{l,a}$ [A]	R_b [Ω]	R_u^* [Ω]	$V_{o,b1}$ [V]
Minimum	0	0.1	0.008	12
Maximum	5	0.5	0.015	16.8

A. Impact of Average Load Current

Fig. 6 shows the efficiencies of the battery semi-active HESS and battery-only system when the average load current, $I_{l,a}$, is enlarged to 3 A and other parameters remain the same. As shown in Fig. 6(a), the area that η_{bo} is greater than η_{bs} becomes larger due to a larger $I_{l,a}$. It explains that given a same Var(i_l), $\Delta\eta$ in (7) decreases when the average load current, $I_{l,a}$, increases. The corresponding Var$(i_l)_{th}$ in (9) for $I_{l,a}$ =3 A is 26, which is consistent with the Fig. 6(b).

B. Impact of Battery Internal Resistance

Fig. 7 shows the efficiencies of the battery semi-active HESS and the battery-only system when the resistances of the battery packs, R_{s1} and R_{s2}, are doubled. In order to ensure V_{bus} in battery-only system is within 12–16.8 V, the maximum and minimum currents of the battery pack are changed to 8 A and -3 A, respectively. As shown in Fig. 7(a), the area that η_{bo} is greater than η_{bs} shrinks due to the enlarged internal resistances of the battery packs. This result well proves that the best usage of ultracapacitors is to combine with batteries with a large internal resistance. The corresponding Var$(i_l)_{th}$ in (9) for $I_{l,a}$ =2 A is 5.9, which is consistent with Fig. 7(b). It shows that Var$(i_l)_{th}$ decreases when $I_{l,a}$ decreases and the

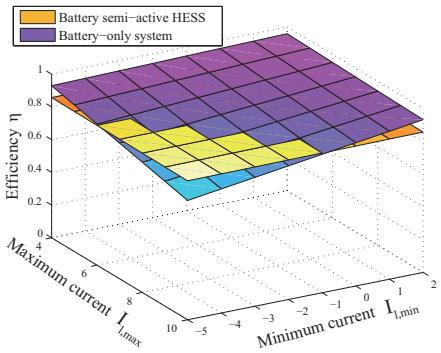

(a)

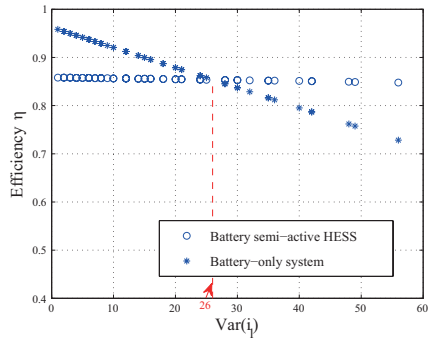

(b)

Fig. 6. Efficiency maps of the battery semi-active HESS and the battery-only system when $I_{l,a}$ =3 A. (a) Efficiency as a function of $I_{l,max}$ and $I_{l,min}$. (b) Efficiency as a function of Var(i_l).

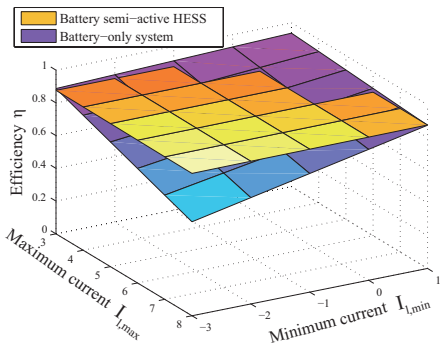

(a)

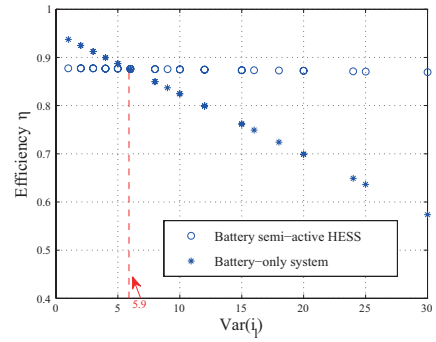

(b)

Fig. 7. Efficiency maps of the battery semi-active HESS and the battery-only system when $I_{l,a}$ =2 A and the internal resistances of the battery packs are doubled. (a) Efficiency as a function of $I_{l,max}$ and $I_{l,min}$. (b) Efficiency as a function of Var(i_l).

battery internal resistances, R_{s1} and R_{s2}, increase. Therefore, the benefit of the battery semi-active HESS over the battery-only system becomes obvious when the internal resistance of the battery pack is large and the load demand has a high peak-to-average ratio.

IV. A Case Study

A. JC08 Driving Cycle

Fig. 8 shows the velocity and power profiles of the JC08 driving cycle. It is the new Japanese urban test cycle that represents a congested city driving. In the JC08 driving cycle, the maximum speed is 81.6 km/h and the average speed is 24.4 km/h. The required load power P can be calculated as

$$P = \left(ma + \mu mg\cos\theta + mg\sin\theta + \frac{1}{2}\rho C_D A v^2 \right) v, \quad (10)$$

where v and a are the vehicle velocity and the acceleration, respectively. The parameters of a compact-size electric vehicle used in this case study are listed in Table III. Fig. 8 shows that the required load power P varies from -12 to 19 kW. The negative power here corresponds to the charge by regenerative braking. The power profile is then scaled down in order to match the power capability of the battery-only system described in Table I. The output current of the DC-DC converter i_d is controlled to supply the average load current $I_{cycle,a}$.

TABLE III
Parameters for a Compact-Size Electric Vehicle

Parameter	Value
m (Vehicle mass)	1,100 kg
C_D (Aerodynamic drag coefficient)	0.24
A (Frontal area)	2.17 m^2
μ (Rolling coefficient)	0.01
ρ (Air density)	1.2 kg/m^3
θ (Road slope angle)	0 degree

The average load current $I_{cycle,a}$ and variance Var(i_{cycle}) of the scaled JC08 driving cycle are approximately calculated as

$$I_{cycle,a} = \frac{1}{N}\sum_{k=1}^{N}\frac{P_{l,k}}{V_{u0}}, \quad (11)$$

$$\mathrm{Var}(i_{cycle}) = \frac{1}{N}\sum_{k=1}^{N}\left(\frac{P_{l,k}}{V_{u0}} - I_{cycle,a}\right)^2, \quad (12)$$

where V_{u0} is the initial voltage of the ultracapacitor pack, which is equal to the initial voltage of the battery pack in the battery-only system. $I_{cycle,a}$ is 0.64 A, and Var(i_{cycle}) is 2.45. The threshold of the load variance Var$(i_{cycle})_{th}$ in (9) is 1.01. Because Var(i_{cycle}) is greater than Var$(i_{cycle})_{th}$, the efficiency of the battery semi-active HESS is higher than that of the battery-only system based on the previous analysis.

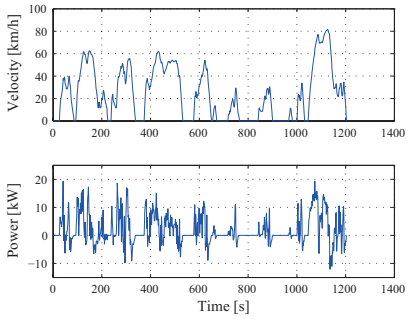

Fig. 8. JC08 velocity and power profiles.

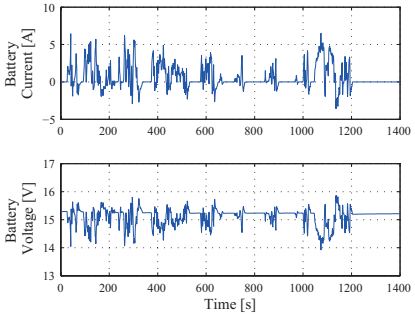

Fig. 9. Simulation results of the battery-only system when initial SOC of the battery pack is 50%.

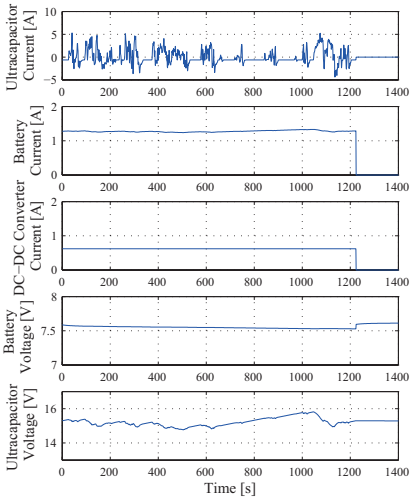

Fig. 10. Simulation results of the battery semi-active HESS when initial SOC of the battery pack is 50%.

TABLE IV
EFFICIENCIES COMPARISON

	$E_{loss,b}$[J]	$E_{loss,d}$[J]	$E_{loss,u}$[J]	η[%]
Battery-only sys.	707.98	N/A	N/A	94.2
HESS	131.34	209.15	136.29	96.0

B. Simulation Result

Simulation models of the battery semi-active HESS in Fig. 3(a) and battery-only system in Fig. 2(a) are built in Matlab/Simulink to investigate the efficiencies and time responses of the two systems. Fig. 9 and 10 show the simulation results of the two systems. The initial SOCs of the battery packs are both set to be 50%. As shown in Table IV, the efficiency of battery semi-active HESS is higher than that of the battery-only system. $E_{loss,b}$, $E_{loss,d}$, and $E_{loss,u}$ are the energy losses in battery pack, DC-DC converter, and ultracpacitor pack, respectively. This result validates the previous theoretical analysis. And the energy loss of the DC-DC converter is the major part of the overall energy loss in the battery semi-active HESS.

Due to the additional ultracapacitor pack and DC-DC converter, the cost of the battery semi-active HESS is higher than that of the battery-only system. However, the life time of the batteries in the battery semi-active HESS can be extended because the peak power demand of batteries in battery semi-active HESS is lower than that of the battery-only system. Since this work only focuses on the efficiencies of the battery-only system and battery semi-active HESS, the cost and cycle life are not discussed here but needed to be considered in practice.

V. CONCLUSION

This paper provides a quantitative and comparative study on efficiencies of the battery semi-active HESS and battery-only system using their ESR circuit models and a pulsed current load. It is theoretically proved that the efficiency difference between the two systems depends on the variance of the load current, the average load current, and the internal resistance of the battery pack. A threshold variance is derived, above which the battery semi-active HESS becomes more energy efficient. This threshold decreases with an increasing internal resistance of the battery pack and/or a decreasing average load current. Therefore, the best usage of ultracapacitors is to combine with batteries designed for low cost (i.e. a large internal resistance), and supply the dynamic part of a current load with a high peak-to-average ratio. And in the HESS, minimizing the energy loss in the DC-DC converter is crucial for a high overall system efficiency. The future work may include the evaluation of efficiencies of the battery semi-active HESS and the battery-only system at various temperatures.

ACKNOWLEDGMENT

The authors would like to thank National Science Foundation of China [grant number 50950110341], for supporting this work.

APPENDIX A
EQUIVALENT SERIES RESISTANCES

A. Battery-only System

As shown in Fig. 2(a), the energy loss in the battery pack is due to R_{s1}, $R_{t1,s}$, and $R_{t1,m}$. Because R_{s1} is much larger than $R_{t1,s}$ and $R_{t1,m}$, the power loss of battery pack $P_{loss,b}$ can be approximately written as

$$P_{loss,b} \approx R_{s1} i_b^2. \quad (13)$$

Thus V_b and ESR R_b in Fig. 2(b) are

$$V_b = V_{o,b1}, \quad (14)$$

$$R_b = \frac{P_{loss,b}}{i_b^2} = R_{s1}, \quad (15)$$

respectively.

B. Battery Semi-active HESS

The energy loss of the battery semi-active HESS includes the losses from the battery pack, the DC-DC converter, and the ultracapacitor pack. Similarly, the energy losses caused by $R_{t2,s}$ and $R_{t2,m}$ are neglected. V_b^* and ESR R_b^* in Fig. 3(b) are calculated using (16) and (17).

$$V_b^* = \frac{V_{o,b2} i_b}{i_d} = \frac{V_{o,b2}}{1-d_s}, \quad (16)$$

$$R_b^* = \frac{P_{loss,b}}{i_d^2} = \frac{i_b^2 R_{s2}}{i_d^2} = \frac{R_{s2}}{(1-d_s)^2}, \quad (17)$$

$$d_s = 1 - \frac{V_{o,b2} + \sqrt{V_{o,b2}^2 - 4R_{in} I_{l,a} V_{o,u}}}{2V_{o,u}},$$

$$R_{in} = R_{s2} + R_{MOS} + R_L,$$

where d_s is the duty cycle of the DC-DC converter. The power loss of the DC-DC converter $P_{loss,d}$ can be approximated using its first-order model, where the switching duty cycle d_s and the average inductor current i_L are used to estimate the losses in MOSFET switches, S_{MOS1}, S_{MOS2}, and inductor L [24], [25]. The resistances of the two MOSFET switches are both R_{MOS} assuming a same type of MOSFET is used. Then the power loss becomes

$$P_{loss,d} = R_{MOS} i_L^2 + R_L i_L^2, \quad (18)$$

where R_L is the resistance of the inductor L. Their parameter values are listed in Table I. As shown in Fig. 3(b), the ESR R_d^* in terms of the current of the DC-DC converter i_d is

$$R_d^* = \frac{P_{loss,d}}{i_d^2} = \frac{R_{MOS} i_L^2 + R_L i_L^2}{i_d^2} = \frac{R_{MOS} + R_L}{(1-d_s)^2}. \quad (19)$$

Because R_{pc} is usually large, the power loss of the ultracapacitor pack $P_{loss,u}$ can be approximately written as

$$P_{loss,u} = R_{sc} i_u^2 + \frac{V_{o,u}^2}{R_{pc}} \approx R_{sc} i_u^2. \quad (20)$$

Thus ESR R_u^* in Fig. 3(b) is written as

$$R_u^* = R_{sc}. \quad (21)$$

REFERENCES

[1] D. Shin, Y. Kim, Y. Wang, N. Chang, and M. Pedram, "Constant-current regulator-based battery-supercapacitor hybrid architecture for high-rate pulsed load applications," *J. Power Sources*, vol. 205, pp. 516–524, May 2012.

[2] A. Khaligh and Z. Li, "Battery, ultracapacitor, fuel cell, and hybrid energy storage systems for electric, hybrid electric, fuel cell, and plug-in hybrid electric vehicles: State of the art," *IEEE Trans. Veh. Technol.*, vol. 59, pp. 2806–2814, Jul. 2010.

[3] A. Kuperman and I. Aharon, "Battery–ultracapacitor hybrids for pulsed current loads: A review," *Renew Sust. Energy Rev.*, vol. 15, pp. 981–992, Feb. 2011.

[4] R. A. Dougal, S. Liu, and R. E. White, "Power and life extension of battery-ultracapacitor hybrids," *IEEE Trans. Compon Packag Technol*, vol. 25, pp. 120–131, Mar. 2002.

[5] G. Sikha and B. N. Popov, "Performance optimization of a battery–capacitor hybrid system," *J. Power Sources*, vol. 134, pp. 130–138, Jul. 2004.

[6] D. Cericola, P. Ruch, R. Kötz, P. Novák, and A. Wokaun, "Simulation of a supercapacitor/li-ion battery hybrid for pulsed applications," *J. Power Sources*, vol. 195, no. 9, pp. 2731–2736, 2010.

[7] C. E. Holland, J. Weidner, R. Dougal, and R. White, "Experimental characterization of hybrid power systems under pulse current loads," *Journal of Power Sources*, vol. 109, no. 1, pp. 32–37, 2002.

[8] L. Gao, R. A. Dougal, and S. Liu, "Power enhancement of an actively controlled battery/ultracapacitor hybrid," *IEEE Trans. Power Electron.*, vol. 20, pp. 236–243, Jan. 2005.

[9] J. Moreno, M. E. Ortúzar, and J. W. Dixon, "Energy-management system for a hybrid electric vehicle, using ultracapacitors and neural networks," *IEEE Trans. Ind. Electron*, vol. 53, pp. 614–623, Apr. 2006.

[10] W.-S. Lin and C.-H. Zheng, "Energy management of a fuel cell/ultracapacitor hybrid power system using an adaptive optimal-control method," *Journal of Power Sources*, vol. 196, pp. 3280–3289, Mar. 2011.

[11] O. Erdinc, B. Vural, and M. Uzunoglu, "A wavelet-fuzzy logic based energy management strategy for a fuel cell/battery/ultra-capacitor hybrid vehicular power system," *J. Power sources*, vol. 194, pp. 369–380, Oct. 2009.

[12] M. Zandi, A. Payman, J.-P. Martin, S. Pierfederici, B. Davat, and F. Meibody-Tabar, "Energy management of a fuel cell/supercapacitor/battery power source for electric vehicular applications," *IEEE Trans. Veh. Technol*, vol. 60, pp. 433–443, Feb. 2011.

[13] D. Rotenberg, A. Vahidi, and I. Kolmanovsky, "Ultracapacitor assisted powertrains: Modeling, control, sizing, and the impact on fuel economy," *IEEE Trans. Control Syst. Technol.*, vol. 19, pp. 576–589, May 2011.

[14] O. Laldin, M. Moshirvaziri, and O. Trescases, "Predictive algorithm for optimizing power flow in hybrid ultracapacitor/battery storage systems for light electric vehicles," *IEEE Trans. Power Electron*, vol. 28, pp. 3882–3895, Aug. 2013.

[15] M.-E. Choi, S.-W. Kim, and S.-W. Seo, "Energy management optimization in a battery/supercapacitor hybrid energy storage system," *IEEE Trans. Smart Grid*, vol. 3, pp. 463–472, Mar. 2012.

[16] H. Yin, C. Zhao, M. Li, and C. Ma, "Optimization based energy control for battery/super-capacitor hybrid energy storage systems," in *Proc. IEEE Industrial Electronics Society, (IECON'2013)*, Vienna, Austria, Nov. 2013, pp. 6764–6769.

[17] J. Cao and A. Emadi, "A new battery/ultracapacitor hybrid energy storage system for electric, hybrid, and plug-in hybrid electric vehicles," *IEEE Trans. Power Electron*, vol. 27, pp. 122–132, Jan. 2012.

[18] A. Kuperman, I. Aharon, S. Malki, and A. Kara, "Design of a semi-active battery-ultracapacitor hybrid energy source," *IEEE Trans. Power Electron*, vol. 28, pp. 806–815, Feb. 2013.

[19] M. Chen and G. A. Rincon-Mora, "Accurate electrical battery model capable of predicting runtime and iv performance," *IEEE Trans. Energy Convers.*, vol. 21, no. 2, pp. 504–511, 2006.

[20] R. C. Kroeze and P. T. Krein, "Electrical battery model for use in dynamic electric vehicle simulations," in *Proc. IEEE Power Electronics Specialists (PESC'2008)*, Rhodes, Greece, Jun. 2008, pp. 1336–1342.

[21] S. Abu-Sharkh and D. Doerffel, "Rapid test and non-linear model characterisation of solid-state lithium-ion batteries," *J. Power Sources*, vol. 130, pp. 266–274, May 2004.

[22] M. S. Chan, K. Chau, and C. Chan, "Effective charging method for ultracapacitors," *Journal of Asian Electric Vehicles*, vol. 3, pp. 771–776, Dec. 2005.

[23] W. Lajnef, J.-M. Vinassa, O. Briat, S. Azzopardi, and E. Woirgard, "Characterization methods and modelling of ultracapacitors for use as peak power sources," *J. Power Sources*, vol. 168, pp. 553–560, Jun. 2007.

[24] Y. Choi, N. Chang, and T. Kim, "DC-DC converter-aware power management for low-power embedded systems," *IEEE Trans. Comput.-Aid. Des.*, vol. 26, pp. 1367–1381, Aug. 2007.

[25] T. Eichhorn, "Boost converter efficiency through accurate calculations," *Power Electron*, vol. 34, pp. 30–35, Sep. 2008.